Hindawi Publishing Corporation
International Journal of Photoenergy
Volume 2012, Article ID 256096, 9 pages
doi:10.1155/2012/256096

Research Article

Preparation of TiO_2-Fullerene Composites and Their Photocatalytic Activity under Visible Light

Ken-ichi Katsumata, Nobuhiro Matsushita, and Kiyoshi Okada

Materials and Structures Laboratory, Tokyo Institute of Technology, 4259 Nagatsuta, Midori-ku, Kanagawa, Yokohama 226-8503, Japan

Correspondence should be addressed to Ken-ichi Katsumata, katsumata.k.ab@m.titech.ac.jp

Received 8 July 2011; Accepted 1 September 2011

Academic Editor: Shifu Chen

The development of visible light-sensitive photocatalytic materials is being investigated. In this study, the anatase and rutile-C_{60} composites were prepared by solution process. The characterization of the samples was conducted by using XRD, UV-vis, FT-IR, Raman, and TEM. The photocatalytic activity of the samples was evaluated by the decolorization of the methylene blue. From the results of the Raman, FT-IR, and XRD, the existence of the C_{60} was confirmed in the samples. The C_{60} was modified on the anatase or rutile particle as a cluster. The C_{60} didn't have the photocatalytic activity under UV and visible light. The anatase and rutile-C_{60} composites exhibited lower photocatalytic activity than the anatase and rutile under UV light. The anatase-C_{60} exhibited also lower activity than the anatase under visible light. On the other hand, the rutile-C_{60} exhibited higher activity than the rutile under visible light. It is considered that the photogenerated electrons can transfer from the C_{60} to the rutile under visible light irradiation.

1. Introduction

Since the photocatalytic activity of a TiO_2 was discovered in 1970s, it has been studied by many researchers because nontoxic, chemical stable, inexpensive, and widely available [1, 2]. When TiO_2 is irradiated by ultraviolet (UV) light, electron (e^-) and hole (h^+) pairs are generated and produce radical species such as OH radicals and O_2^- by reaction with moisture in the atmosphere, which reduce and oxidize adsorbates on the surface. These radicals can decompose most organic compounds and bacteria [3–7]. Therefore, the photocatalyst has been applied on various industrial fields [8, 9]. However, since the band gap of TiO_2 is 3.0–3.2 eV, the TiO_2 photocatalyst is activated only by UV light irradiation (<400 nm) [10].

To exhibit the photocatalytic activity under visible light, metal (Cr, V, Fe, Mn, Co, and Ni) doping into Ti site and anion (N, S, and C) doping into O site have been studied [11–20]. These doped TiO_2 can be sensitive to visible light, but the oxidative power of holes decreases. Because the holes are generated in a localized narrow band originating from the dopant metal ions or anions in the forbidden band of TiO_2. Recently, it has been reported that TiO_2 powders with grafted metal ions (Cu(II), Cr(III), Ce(III), and Fe(III)) were capable of serving as photocatalysts sensitive to visible light [21–25]. This system is called the interfacial charge transfer (IFCT) and has greatly an oxidative decomposition activity.

Among these materials, carbon-supported TiO_2 also exhibited the photocatalytic activity under visible light [26–30]. Fullerene (C_{60}) has the interesting properties which are the delocalized conjugated structures and electron-accepting ability. C_{60} can efficiently promote a rapid photoinduced charge separation and slow charge recombination. Although the role of C_{60}, accepting the photogenerated electrons from TiO_2 particles, has been demonstrated, a few efforts are made to utilize the unique properties of C_{60} to increase the efficiency of photocatalysis [31, 32]. However, the mechanism is not clear in detail.

In this study, TiO_2-C_{60} composites were prepared and characterized, and the photocatalytic activity under UV and visible light was evaluated, comparing to the pure TiO_2. The mechanism of visible light-sensitive photocatalyst was investigated by using the photodeposition of platinum (Pt).

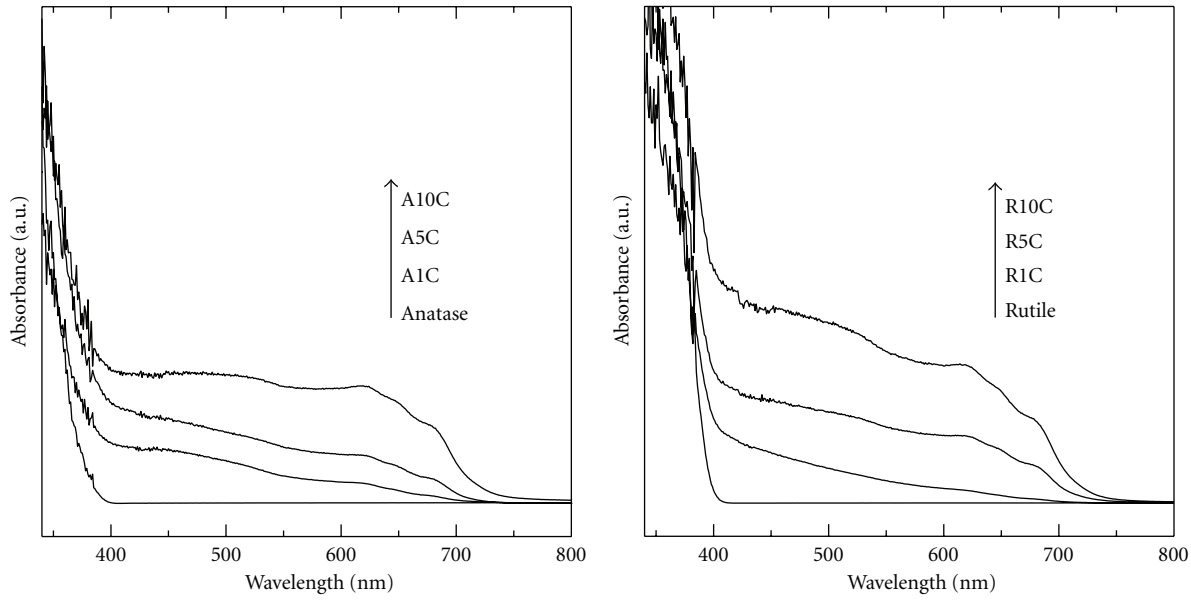

Figure 1: UV-vis spectra of the samples. (a) The anatase, A1C, A5C, and A10C samples, (b) the rutile, R1C, R5C, and R10C samples.

2. Experimental

2.1. Preparation of TiO_2-Fullerene Composites. Fullerene (C_{60}) solution was prepared by adding C_{60} (1, 5, 10 mg) into toluene (30 mL) and mixing for 10 min. TiO_2 powder (anatase or rutile; 100 mg) was put in the solution, and it was mixed at 80°C for 24 hours. Then, the solution was evaporated and dried at 90°C, and the TiO_2-C_{60} composite samples were obtained. The anatase powder and toluene were taken from Wako Pure Chemical Industries, Tokyo, Japan. The C_{60} (carbon cluster; ST) was taken from Kanto Chemicals Co. Inc., Tokyo, Japan. The rutile powder (MT-150A) was taken from TAYCA Co., Tokyo, japan. The samples with different C_{60}-additive amount are denoted in this report as "AXC or RXC." A, R, X, and C indicate the anatase, rutile, C_{60} additive amount, and C_{60}, respectively. For example, A1C means 1 mass % C_{60} added anatase sample.

2.2. Synthesis of Photodeposited Samples. The prepared TiO_2-fullerene composite samples were dispersed in 3 : 7 (v/v) methanol/water solution (20 mL), and then the required amount (5 mass%) H_2PtCl_6 solution was added in. The mixture was irradiated by fluorescent light with cut filter (>420 nm) for 3 hours at room temperature. After irradiation, the sample was collected by centrifugation and washed several times with distilled water. The obtained paste was dried at 80°C.

2.3. Characterization of the Samples. The crystalline phases were identified by a high-power X-ray diffractometer (XRD, RINT-TTR3B; Rigaku, Japan) using monochromated Cu Kα radiation (50 kV–200 mA). The samples were analyzed using a Raman spectroscopy (RAMANOR T64000; Jobin-Yvon S.A.S., France) with an Ar laser (514.5 nm) operated at 50 mW. UV-visible absorption properties of the samples were measured using a UV-visible scanning spectrophotometer (UV-vis, Lambda 35; PerkinElmer Inc., USA). Transmission electron microscopy (TEM) observation of the samples was performed using a transmission electron microscope (TEM, HF-2000, Hitachi, Japan) operating at 200 kV. For TEM observation, one drop of the sample, dispersed in water, was deposited on an amorphous carbon grid. IR measurements were performed using a Fourier transform-infrared spectroscopy (FT-IR, JIR-7000, JEOL, Japan).

2.4. Evaluation of Photocatalytic Activity. Photocatalytic activity of the samples was evaluated by decomposition of methylene blue (MB; $C_{16}H_{18}ClN_3S$). The samples were immersed in 0.02 mM MB aqueous solution for overnight to saturate the adsorption. After washing by ultrapure water, a cylinder (ϕ40 × 30 mm) was contacted on the SiO_2 glass (50 × 50 × 2t mm) by using silicone grease, and 0.01 mM MB aqueous solution was poured into the cylinder. And then, the samples (0.05 g) were put into the solution. Irradiating overhead UV light (1.0 mW/cm^2) or fluorescent light (10,000 lx), the absorption spectra of MB were measured by a UV-vis spectrophotometer.

3. Results and Discussion

3.1. Characterization of the TiO_2-C_{60} Composite Samples. Anatase and rutile were white powders because they cannot absorb the wavelength in visible range. The obtained sample with C_{60}, however, had a color. With increasing C_{60}-additive amount, the color of the samples became gray. Figure 1 shows the UV-vis absorption spectra of the samples. The adsorption of anatase and rutile started from <400 nm. On the other hand, the sample with C_{60} adsorbed the photon of

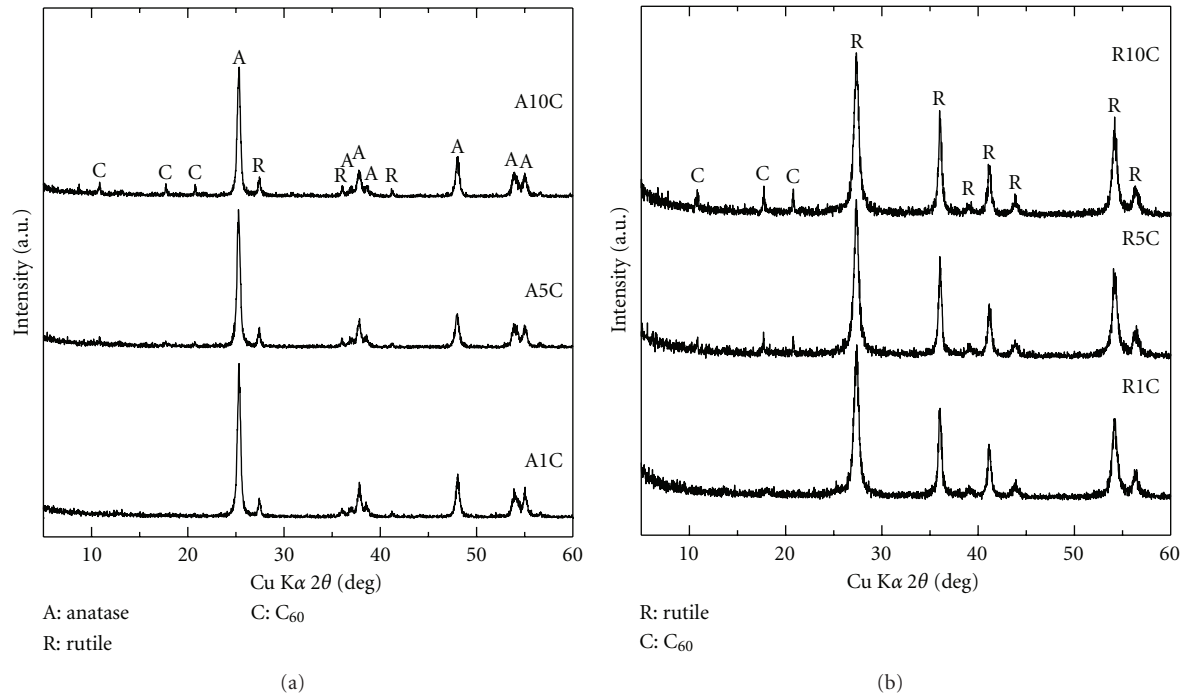

Figure 2: XRD patterns of the TiO_2-C_{60} composite samples. (a) The A1C, A5C, and A10C samples, (b) the R1C, R5C, and R10C samples.

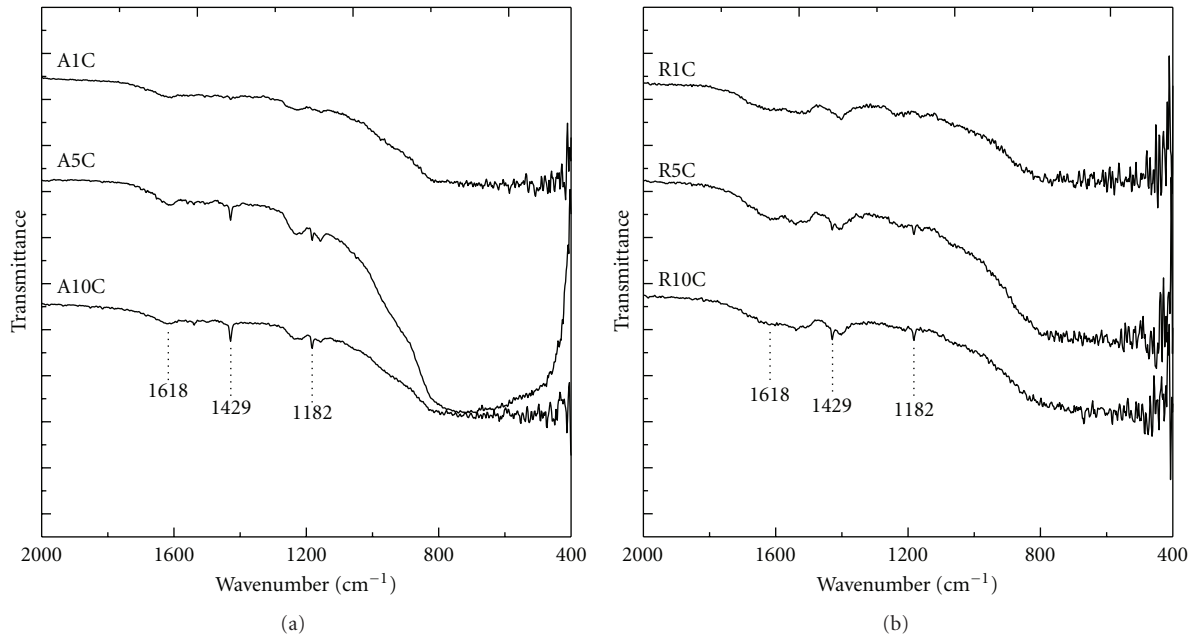

Figure 3: IR spectra of the TiO_2–C_{60} composite samples. (a) the A1C, A5C, and A10C samples, (b) the R1C, R5C, and R10C samples.

>400 nm, and the adsorption edge was about 700 nm. This is indicated that the sample with C_{60} had absorption property in visible range. The spectrum shape of the sample with C_{60} was similar to the C_{60}, and the absorption increased with increasing C_{60}-additive amount. Therefore, it is considered that the absorption in visible range is attributed to the C_{60}.

Figure 2 shows the XRD patterns of the samples. The crystalline phases detected in the anatase composite samples were anatase, rutile, and C_{60} (Figure 2(a)). Rutile was a little included in the anatase composite sample. This is attributed to the starting materials (chemical), and it was not formed during preparation process of the anatase-C_{60} composite samples. The C_{60} peaks of the A1C sample were not seen clearly, but the peaks appeared in the A5C and A10C samples. In the case of the rutile composite samples, the crystalline phases were rutile and C_{60}, and anatase was

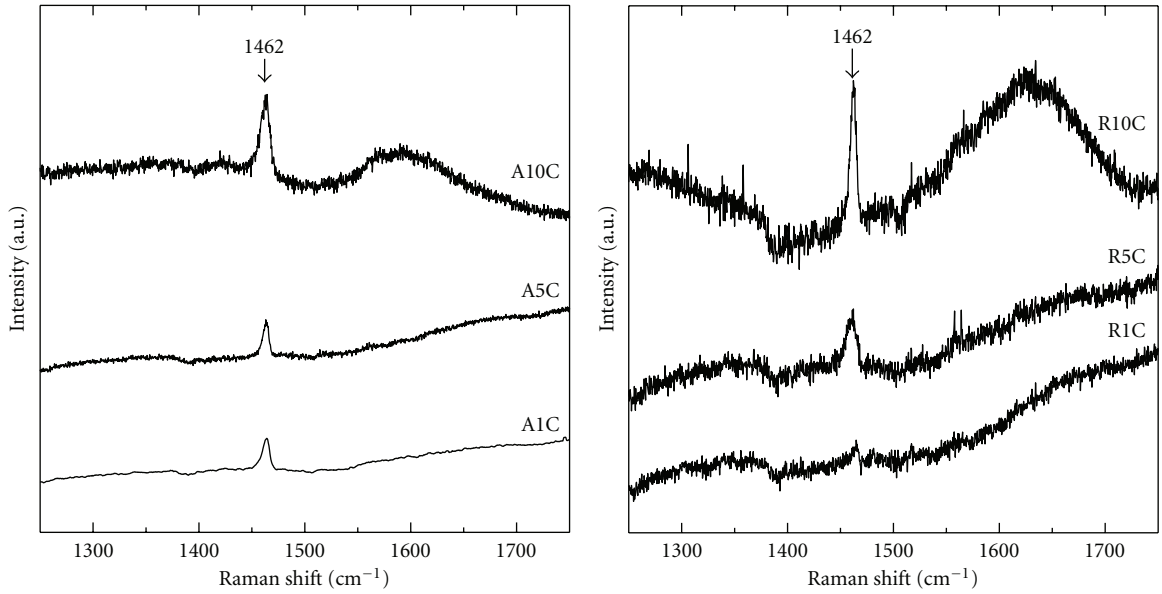

Figure 4: Raman spectra of the TiO_2–C_{60} composite samples. (a) The A1C, A5C, and A10C samples, (b) the R1C, R5C, and R10C samples.

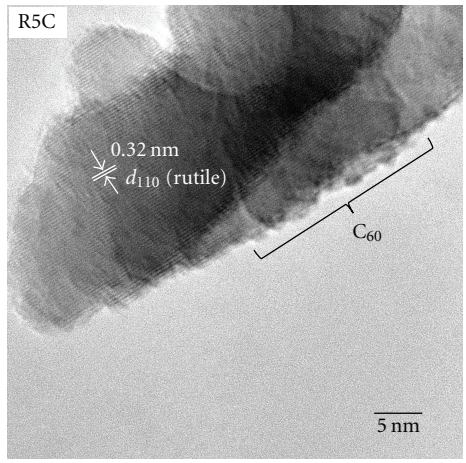

Figure 5: High resolution TEM image of the R5C samples.

not included (Figure 2(b)). The C_{60} peaks of the R1C sample were not seen clearly, but the peaks appeared in the R5C and R10C samples. This is the similar tendency in the anatase composite samples. In both cases, the values of the full width at half maximum (FWHM) in the anatase (101) peak (2θ = 25.32°) and rutile (110) peak (2θ = 27.44°) were almost the same, respectively. This is indicated that the crystallinity of the anatase or rutile composite samples have almost the same crystallinity, respectively.

Figure 3 shows the IR adsorption spectra of the samples measured in air at room temperature. In the infrared bands of C_{60}, there are the four most intense lines at 1429, 1183, 577, and 528 cm^{-1} [33, 34]. The absorption bands at 1429 and 1183 cm^{-1} were observed in A5C, A10C, R5C, and R10C samples, but those were not observed in A1C and R1C samples (Figures 3(a) and 3(b)). The adsorption bands at 577 and 528 cm^{-1} were not seen in all samples because widely adsorption of TiO_2 was at 400–900 cm^{-1}. On the other hand, the adsorption band at 1618 cm^{-1} was seen in all samples. This is attributed to the bending vibration of the H_2O molecule adsorbed on Ti^{4+} site [35].

The Raman spectra of the samples are shown in Figure 4. The peak at 1642 cm^{-1} appeared in all samples (Figures 4(a) and 4(b)). Cataldo [36] reported that the Raman spectrum of pure C_{60} is characterized by several lines, the most intense which are the $A_g(1)$ and $A_g(2)$ modes lying, respectively, at 496 and at 1469 cm^{-1}. The $A_g(2)$ mode is also referred as the pentagonal pinch mode. It is considered that the peak observed at 1642 cm^{-1} is $A_g(2)$ mode of C_{60}. The existence of the C_{60} in A1C and R1C samples could not be detected by XRD and IR, but it could be confirmed by the Raman spectra. In A10C and R10C samples, the broad band at around 1600 cm^{-1} appeared. It is guessed that the band is attributed to the carbon cluster.

Figure 5 shows the high resolution TEM image of the R5C sample. Considering the space of the lattice fringe, the particle was confirmed to rutile. Some small particles were observed at the edge of the rutile particle. In the case of the anatase-C_{60} composite samples, the small particles were also observed at the edge of the anatase particles (not shown here). These particles were not the rutile and anatase particles. It is guessed that these small particles are the C_{60} particles adhered to the rutile particles. In the TiO_2-C_{60} composite samples, we consider that the C_{60} particles are directly present on the surface of the TiO_2 particles.

3.2. Evaluation of the Photocatalytic Activity of the TiO_2-C_{60} Composite Samples. Figure 6 shows the photocatalytic degradation of MB in the C_{60}. If the C_{60} has photocatalytic

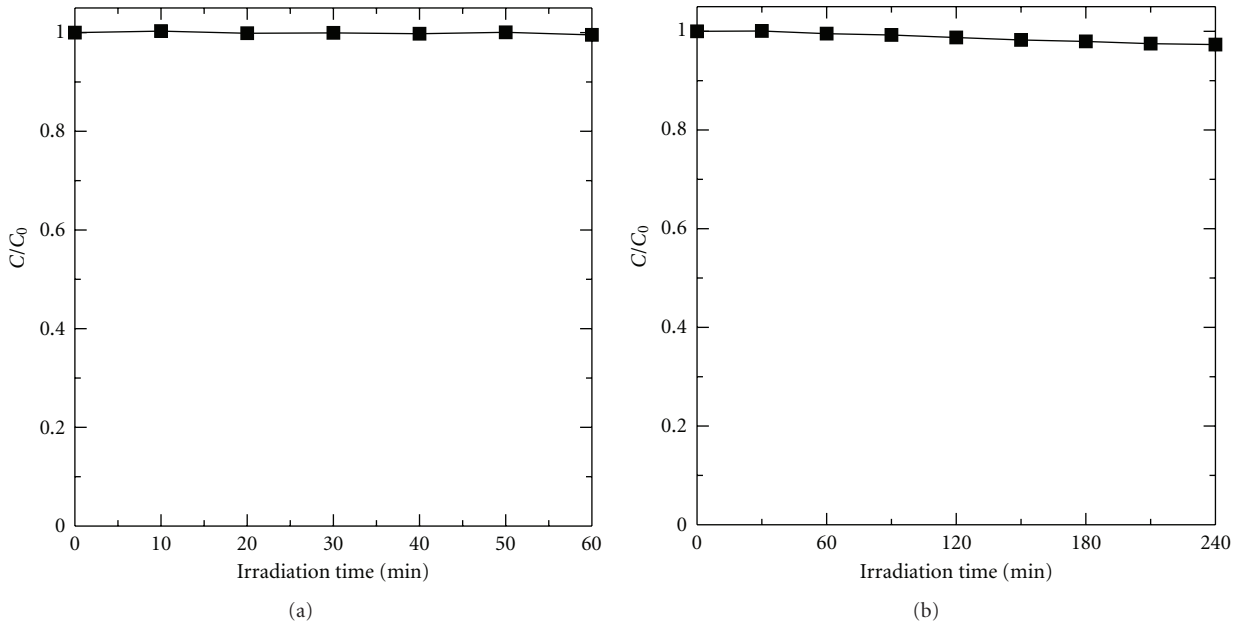

FIGURE 6: Changes of the MB concentrations decomposed by the C_{60} as a function of (a) UV irradiation time (1.0 mW/cm^2), (b) visible light irradiation time (10,000 lx).

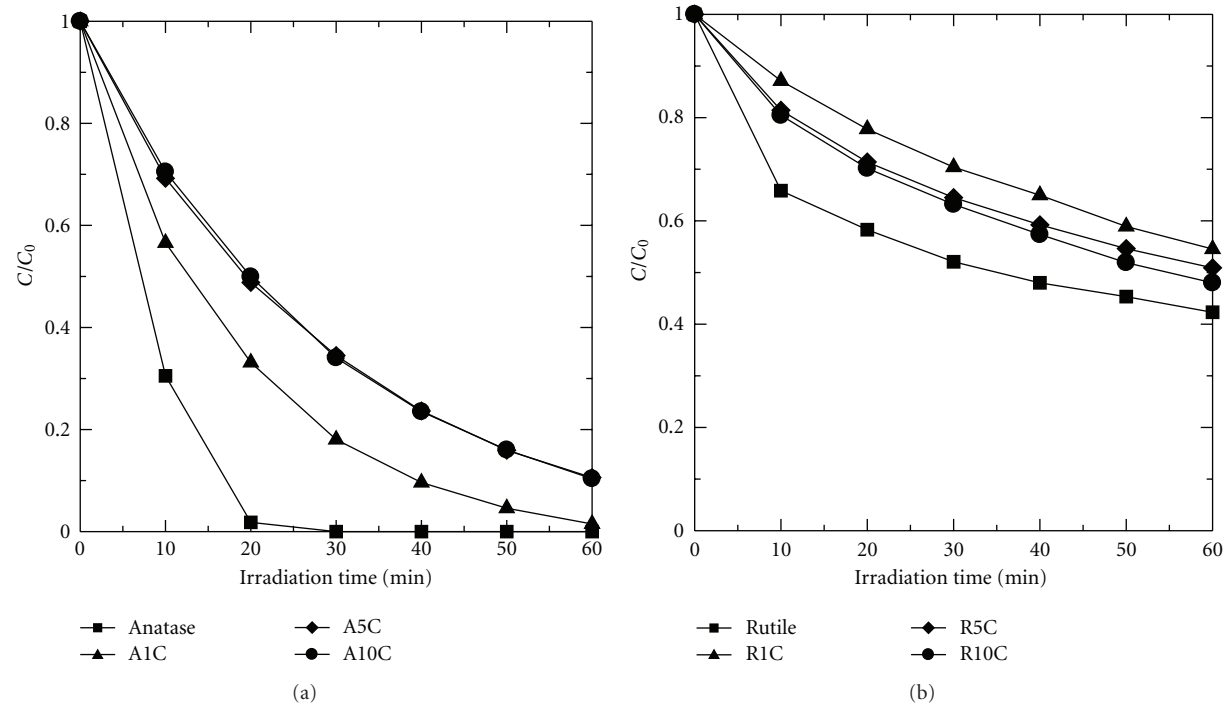

FIGURE 7: Changes of the MB concentrations decomposed by the samples as a function of UV irradiation time (1.0 mW/cm^2). (a) The anatase, A1C, A5C, and A10C samples, (b) The rutile, R1C, R5C, and R10C samples.

activity, MB is decolorized. Figure 6(a) shows the test under UV irradiation. When UV irradiation time increased, the variation of the MB concentration was little. This result indicates that the C_{60} has little photocatalytic activity under UV light irradiation. The MB concentration slightly decreased with increasing visible light irradiation time (Figure 6(b)). However, the decrement of the MB concentration was a little. It is considered that the C_{60} exhibited little the photocatalytic activity under UV and visible light.

Figure 7 shows the photocatalytic degradation of MB in the anatase, rutile, and anatase or rutile-C_{60} composite samples under UV irradiation. When UV irradiation time

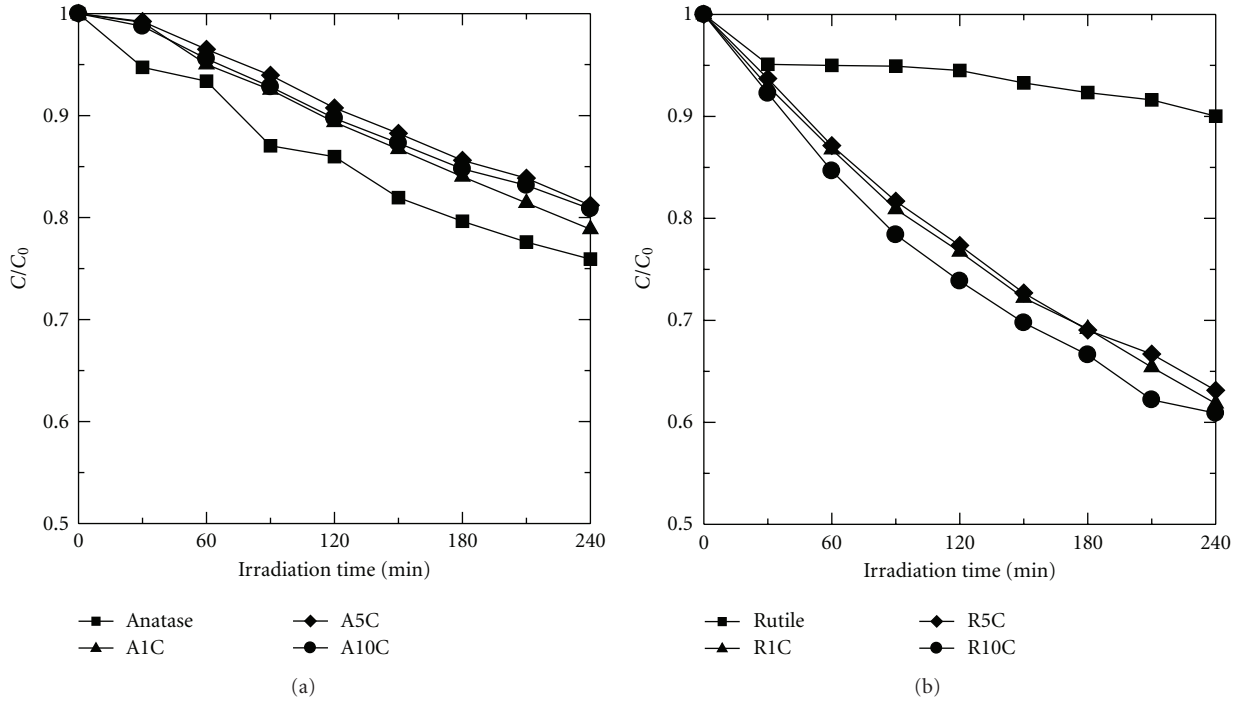

Figure 8: Changes of the MB concentrations decomposed by the samples as a function of visible light irradiation time (10,000 lx). (a) The anatase, A1C, A5C, and A10C samples, (b) The rutile, R1C, R5C, and R10C samples.

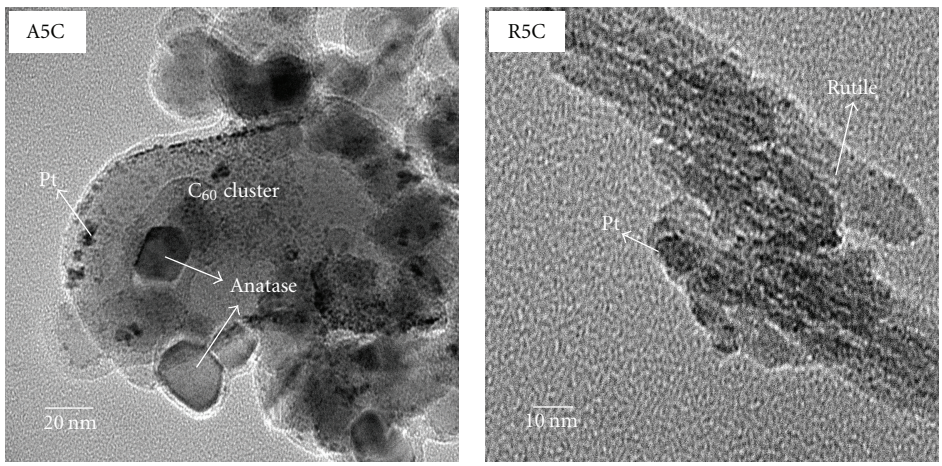

Figure 9: TEM images of the A5C and R5C samples after the photodeposition of Pt particles.

increased, the MB concentration of the anatase, A1C, A5C, and A10C samples decreased (Figure 7(a)). Among them, the MB concentration of the anatase decreased drastically. This result indicates that the photocatalytic activity of the A1C, A5C, and A10C samples is lower than that of the anatase. The activity of the A1C sample was higher than that of the A5C and A10C samples, and the A5C sample indicates a similar tendency to the A10C sample. With increasing the C_{60} additive amount, the activity was lower in the anatase-C_{60} composite samples. In the case of the rutile and rutile-C_{60} composite samples, the decrement of the MB concentration in the rutile became the largest (Figure 7(b)). This is indicated that the photocatalytic activity of the rutile is higher than that of the rutile with the C_{60} (R1C, R5C, and R10C samples). The activity of the R10C sample was higher than that of the R1C and R5C samples, and the R5C sample was higher than the R1C sample. The tendency was different from the anatase-C_{60} composite samples. The anatase and rutile-C_{60} composite samples exhibit lower photocatalytic activity under UV irradiation than anatase and rutile. It is guessed that the anatase and rutile surfaces are covered by the C_{60}, and the number of absorbed photons in the anatase and rutile decreases.

Figure 8 shows the photocatalytic degradation of MB in the anatase, rutile, and anatase or rutile-C_{60} composite samples under visible light irradiation. In Figures 8(a) and 8(b), the MB concentration of the anatase and rutile decreased with increasing visible light irradiation time. This result indicates that the anatase and rutile have the photocatalytic activity under visible light irradiation. This is because fluorescent light was used as a light source, so a little UV light was included in the light source. All samples exhibited the photocatalytic activity under visible light irradiation shown in Figure 8(a). But the activity of the A1C, A5C, and A10C samples was lower than the anatase. This is similar tendency to the case of UV irradiation (Figure 7(a)). On the other hand, the R1C, R5C, and R10C samples exhibited higher photocatalytic activity than the rutile (Figure 8(b)). This result indicates that the rutile-C_{60} composite samples have greatly the photocatalytic activity under visible light.

The band structures of the anatase, rutile, and C_{60} are shown in Scheme 1. In the case of the C_{60}, some researchers reported different band structures [37, 38]. The conduction band (CB) positions of the C_{60} were higher energy than those of the anatase and rutile. Therefore, it is prospective that the photogenerated electrons transfer from the CB of the C_{60} to the CB of the anatase and rutile, and the anatase and rutile-C_{60} composite samples have a higher photocatalytic activity than the anatase and rutile under visible light shown in Scheme 2. However, the anatase-C_{60} composite samples exhibited higher photocatalytic activity under visible light than the anatase (Figure 8(a)).

Figure 9 shows the TEM images of the A5C and R5C samples after conducting the photodeposition of Pt under visible light irradiation. In the case of A5C sample, the photodeposited Pt particles were not observed at the anatase particles but the C_{60} cluster. This is indicated that the photogenerated electrons cannot transfer from the C_{60} to the anatase (Scheme 3(a)). On the other hand, in the case of the R5C sample, the photodeposited Pt particles were observed at the rutile. This result indicates that the photogenerated electrons can transfer from the C_{60} to the rutile (Scheme 3(b)). Therefore, it is considered that the rutile-C_{60} composite samples exhibit the photocatalytic activity under visible light.

From the band structure shown in Scheme 1, it is possible that the photogenerated electrons transfer from the C_{60} to the anatase. In this study, however, it did not occur. It is guessed that the connecting state between the C_{60} and the anatase is one of the reasons why the photogenerated electrons cannot transfer from the C_{60} to the anatase. Further investigation is needed to clear the reasons.

Photocatalytic activity of the C_{60}-rutile composite sample was superior to the C_{60}-anatase sample under visible light (Figure 7). On the other hand, the C_{60}-rutile sample exhibited lower activity than the C_{60}-anatase sample under UV light (Figure 8). In this study, the number of photons absorbed to the samples was not uniformed in UV and visible lights shown in UV-visible absorption spectra (Figure 1). It is, therefore, difficult to compare the photocatalytic activities of the C_{60}-anatase and C_{60}-rutile samples under UV-visible light. However, the photocatalytic degradation rate of MB was greatly different between under UV and visible lights, and the rate under UV light was higher than that under visible light. It is guessed that the C_{60}-anatase sample exhibits higher activity than the C_{60}-rutile under UV-visible light.

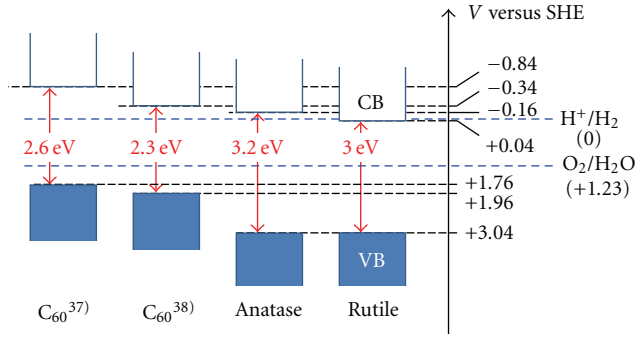

Scheme 1: Schematic illustrations of the band structures of the anatase, rutile, and C_{60}.

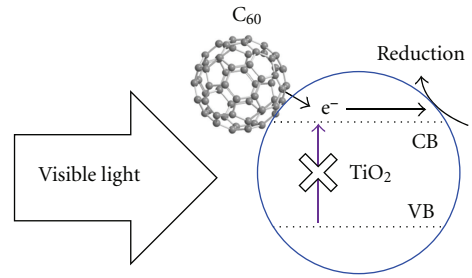

Scheme 2: Schematic illustration of the photogenerated electron transfer model of the TiO_2-C_{60} composite under visible light irradiation.

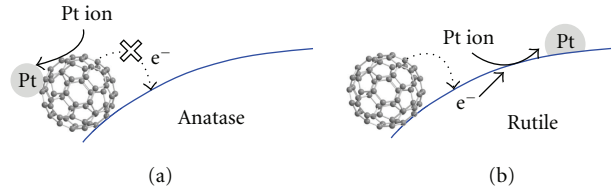

Scheme 3: Schematic illustrations of the photodeposition model of Pt particles on (a) the anatase-C_{60} composite and (b) the rutile-C_{60} composite under visible light irradiation.

4. Conclusions

In present study, the anatase and rutile-C_{60} composites were prepared, and the photocatalytic activity of the composites was investigated by the MB decolorization test. The C_{60} particles were directly adhered to the surface of the TiO_2 particles. When UV light was irradiated, the photocatalytic activity of the anatase and rutile-C_{60} composites became lower than the anatase and rutile particles without the C_{60}. In the case of the visible light irradiation, the anatase-C_{60} composite exhibited also lower activity than the anatase. However, the rutile-C_{60}

composite exhibited higher activity than the rutile. From the photodeposition of Pt on the composites under visible light, the photogenerated electron transfer from the C_{60} to the rutile occurred although the electron transfer did not occur in the anatase-C_{60} composite. Therefore, the rutile-C_{60} composite exhibits the photocatalytic activity under visible light. The rutile-C_{60} can be utilized for the new type of visible light sensitive photocatalyst.

Acknowledgments

The authors are grateful to Mr. Y. Komatsubata in Tokyo Institute of Technology for the HR-TEM observation. This work was supported, in part, by a "Grant-in-Aid for Cooperative Research Project of Nationwide Joint-Use Research Institutes on Advanced Materials Development and Integration of Novel Structured Metallic and Inorganic Materials" and "Inamori Foundation."

References

[1] A. Fujishima and K. Honda, "Electrochemical photolysis of water at a semiconductor electrode," *Nature*, vol. 238, no. 5358, pp. 37–38, 1972.

[2] A. Fujishima, T. N. Rao, and D. A. Tryk, "Titanium dioxide photocatalysis," *Journal of Photochemistry and Photobiology C*, vol. 1, no. 1, pp. 1–21, 2000.

[3] T. Kawai and T. Sakata, "Conversion of carbohydrate into hydrogen fuel by a photocatalytic process," *Nature*, vol. 286, no. 5772, pp. 474–476, 1980.

[4] J. Schwitzgebel, J. G. Ekerdt, H. Gerischer, and A. Heller, "Role of the oxygen molecule and of the photogenerated electron in TiO_2-photocatalyzed air oxidation reactions," *Journal of Physical Chemistry*, vol. 99, no. 15, pp. 5633–5638, 1995.

[5] K. Sunada, T. Watanabe, and K. Hashimoto, "Studies on photokilling of bacteria on TiO_2 thin film," *Journal of Photochemistry and Photobiology A*, vol. 156, no. 1–3, pp. 227–233, 2003.

[6] K. Sunada, Y. Kikuchi, K. Hashimoto, and A. Fujishima, "Bactericidal and detoxification effects of TiO_2 thin film photocatalysts," *Environmental Science and Technology*, vol. 32, no. 5, pp. 726–728, 1998.

[7] C. C. Trapalis, P. Keivanidis, G. Kordas et al., "$TiO_2(Fe^{3+})$ nanostructured thin films with antibacterial properties," *Thin Solid Films*, vol. 433, no. 1-2, pp. 186–190, 2003.

[8] A. Mills and S. L. Hunte, "An overview of semiconductor photocatalysis," *Journal of Photochemistry and Photobiology A*, vol. 108, no. 1, pp. 1–35, 1997.

[9] A. Fujishima, K. Hashimoto, and T. Watanabe, *TiO_2 Photocatalyst, Fundamentals and Applications*, BKC Inc., Tokyo, Japan, 1999.

[10] A. Heller, "Chemistry and applications of photocatalytic oxidation of thin organic films," *Accounts of Chemical Research*, vol. 28, no. 12, pp. 503–508, 1995.

[11] E. Borgarello, J. Kiwi, M. Grätzel, E. Pelizzetti, and M. Visca, "Visible light induced water cleavage in colloidal solutions of chromium-doped titanium dioxide particles," *Journal of the American Chemical Society*, vol. 104, no. 11, pp. 2996–3002, 1982.

[12] M. Anpo and M. Takeuchi, "Design and development of second-generation titanium oxide photocatalysts to better our environment—approaches in realizing the use of visible light," *International Journal of Photoenergy*, vol. 3, no. 2, pp. 89–94, 2001.

[13] T. Umebayashi, T. Yamaki, H. Itoh, and K. Asai, "Analysis of electronic structures of 3d transition metal-doped TiO_2 based on band calculations," *Journal of Physics and Chemistry of Solids*, vol. 63, no. 10, pp. 1909–1920, 2002.

[14] R. Asahi, T. Morikawa, T. Ohwaki, K. Aoki, and Y. Taga, "Visible-light photocatalysis in nitrogen-doped titanium oxides," *Science*, vol. 293, no. 5528, pp. 269–271, 2001.

[15] H. Irie, Y. Watanabe, and K. Hashimoto, "Nitrogen-concentration dependence on photocatalytic activity of $TiO_{2-x}N_x$ powders," *Journal of Physical Chemistry B*, vol. 107, no. 23, pp. 5483–5486, 2003.

[16] H. Irie, S. Washizuka, Y. Watanabe, T. Kako, and K. Hashimoto, "Photoinduced hydrophilic and electrochemical properties of nitrogen-doped TiO_2 films," *Journal of the Electrochemical Society*, vol. 152, no. 11, pp. E351–E356, 2005.

[17] T. Umebayashi, T. Yamaki, H. Itoh, and K. Asai, "Band gap narrowing of titanium dioxide by sulfur doping," *Applied Physics Letters*, vol. 81, no. 3, pp. 454–456, 2002.

[18] T. Ohno, T. Mitsui, and M. Matsumura, "Photocatalytic activity of S-doped TiO_2 photocatalyst under visible light," *Chemistry Letters*, vol. 32, no. 4, pp. 364–365, 2003.

[19] M. Mrowetz, W. Balcerski, A. J. Colussi, and M. R. Hoffmann, "Oxidative power of nitrogen-doped TiO_2 photocatalysts under visible illumination," *Journal of Physical Chemistry B*, vol. 108, no. 45, pp. 17269–17273, 2004.

[20] R. Nakamura, T. Tanaka, and Y. Nakato, "Mechanism for visible light responses in anodic photocurrents at N-doped TiO_2 film electrodes," *Journal of Physical Chemistry B*, vol. 108, no. 30, pp. 10617–10620, 2004.

[21] H. Irie, S. Miura, R. Nakamura, and K. Hashimoto, "A novel visible-light-sensitive efficient photocatalyst, Cr^{III}-grafted TiO_2," *Chemistry Letters*, vol. 37, no. 3, pp. 252–253, 2008.

[22] H. Irie, S. Miura, K. Kamiya, and K. Hashimoto, "Efficient visible light-sensitive photocatalysts: grafting Cu(II) ions onto TiO_2 and WO_3 photocatalysts," *Chemical Physics Letters*, vol. 457, no. 1–3, pp. 202–205, 2008.

[23] H. Irie, K. Kamiya, T. Shibanuma et al., "Visible light-sensitive Cu(II)-grafted TiO_2 photocatalysts: activities and X-ray absorption fine structure analyses," *Journal of Physical Chemistry C*, vol. 113, no. 24, pp. 10761–10766, 2009.

[24] R. Nakamura, A. Okamoto, H. Osawa, H. Irie, and K. Hashimoto, "Design of all-inorganic molecular-based photocatalysts sensitive to visible light: Ti(IV)-O-Ce(III) bimetallic assemblies on mesoporous silica," *Journal of the American Chemical Society*, vol. 129, no. 31, pp. 9596–9597, 2007.

[25] H. Yu, H. Irie, Y. Shimodaira et al., "An efficient visible-light-sensitive Fe(III)-grafted TiO_2 photocatalyst," *Journal of Physical Chemistry C*, vol. 114, no. 39, pp. 16481–16487, 2010.

[26] P. V. Kamat, M. Gevaert, and K. Vinodgopal, "Photochemistry on semiconductor surfaces. Visible light induced oxidation of C_{60} on TiO_2 nanoparticles," *Journal of Physical Chemistry B*, vol. 101, no. 22, pp. 4422–4427, 1997.

[27] W. C. Oh, A. R. Jung, and W. B. Ko, "Characterization and relative photonic efficiencies of a new nanocarbon/TiO_2 composite photocatalyst designed for organic dye decomposition and bactericidal activity," *Materials Science and Engineering C*, vol. 29, no. 4, pp. 1338–1347, 2009.

[28] L. Brunet, D. Y. Lyon, E. M. Hotze, P. J. J. Alvarez, and M. R. Wiesner, "Comparative photoactivity and antibacterial properties of C_{60} fullerenes and titanium dioxide nanoparticles,"

Environmental Science and Technology, vol. 43, no. 12, pp. 4355–4360, 2009.

[29] V. Apostolopoulou, J. Vakros, C. Kordulis, and A. Lycourghiotis, "Preparation and characterization of [60] fullerene nanoparticles supported on titania used as a photocatalyst," *Colloids and Surfaces A*, vol. 349, no. 1–3, pp. 189–194, 2009.

[30] Z. D. Meng, L. Zhu, J. G. Choi, M. L. Chen, and W. C. Oh, "Effect of Pt treated fullerene/TiO_2 on the photocatalytic degradation of MO under visible light," *Journal of Materials Chemistry*, vol. 21, no. 21, pp. 7596–7603, 2011.

[31] V. Krishna, N. Noguchi, B. Koopman, and B. Moudgil, "Enhancement of titanium dioxide photocatalysis by water-soluble fullerenes," *Journal of Colloid and Interface Science*, vol. 304, no. 1, pp. 166–171, 2006.

[32] Y. Long, Y. Lu, Y. Huang et al., "Effect of C_{60} on the photocatalytic activity of TiO_2 nanorods," *Journal of Physical Chemistry C*, vol. 113, no. 31, pp. 13899–13905, 2009.

[33] W. Kratschmer, L. D. Lamb, K. Fostiropoulos, and D. R. Huffman, "Solid C_{60}: a new form of carbon," *Nature*, vol. 347, no. 6291, pp. 354–358, 1990.

[34] W. Krätschmer, K. Fostiropoulos, and D. R. Huffman, "The infrared and ultraviolet absorption spectra of laboratory-produced carbon dust: evidence for the presence of the C_{60} molecule," *Chemical Physics Letters*, vol. 170, no. 2-3, pp. 167–170, 1990.

[35] C. Morterra, "An infrared spectroscopic study of anatase properties. Part 6. Surface hydration and strong Lewis acidity of pure and sulphate-doped preparations," *Journal of the Chemical Society, Faraday Transactions 1*, vol. 84, no. 5, pp. 1617–1637, 1988.

[36] F. Cataldo, "Raman spectra of C_{60} fullerene photopolymers prepared in solution," *European Polymer Journal*, vol. 36, no. 3, pp. 653–656, 2000.

[37] R. Mitsumoto, T. Araki, E. Ito et al., "Electronic structures and chemical bonding of fluorinated fullerenes studied by NEXAFS, UPS, and vacuum-UV absorption spectroscopies," *Journal of Physical Chemistry A*, vol. 102, no. 3, pp. 552–560, 1998.

[38] N. S. Sariciftci, "Polymeric photovoltaic materials," *Current Opinion in Solid State and Materials Science*, vol. 4, no. 4, pp. 373–378, 1999.